Geophysical Research Letters

RESEARCH LETTER
10.1029/2023GL106395

El Niño-La Niña Asymmetries in the Changes of ENSO Complexities and Dynamics Since 1990

Xumin Li[1,2], Jin-Yi Yu[2], and Ruiqiang Ding[3]

[1]Key Laboratory of Meteorological Disaster of Ministry of Education (KLME), Nanjing University of Information Science and Technology, Nanjing, China, [2]Department of Earth System Science, University of California, Irvine, CA, USA, [3]Key Laboratory of Environmental Change and Natural Disasters of Chinese Ministry of Education, Beijing Normal University, Beijing, China

Key Points:

- El Niño-Southern Oscillation complexity underwent significant asymmetric changes around 1990, especially in spatial pattern and temporal evolution
- El Niño's pattern shifted from Eastern Pacific to Central Pacific, while La Niña's timing transitioned from single-year to multi-year
- El Niño's primary dynamic shifted from Tropical Pacific to Subtropical Pacific (SP) whereas La Niña consistently remained in the SP

Supporting Information:

Supporting Information may be found in the online version of this article.

Correspondence to:

J.-Y. Yu,
jyyu@uci.edu

Citation:

Li, X., Yu, J.-Y., & Ding, R. (2024). El Niño-La Niña asymmetries in the changes of ENSO complexities and dynamics since 1990. *Geophysical Research Letters*, *51*, e2023GL106395. https://doi.org/10.1029/2023GL106395

Received 13 SEP 2023
Accepted 11 MAR 2024

Abstract In around 1990, significant shifts occurred in the spatial pattern and temporal evolution of the El Niño-Southern Oscillation (ENSO), with these shifts showing asymmetry between El Niño and La Niña phases. El Niño transitioned from the Eastern Pacific (EP) to the Central Pacific (CP) type, while La Niña's multi-year (MY) events increased. These changes correlated with shifts in ENSO dynamics. Before 1990, El Niño was influenced by the Tropical Pacific (TP) ENSO dynamic, shifting to the Subtropical Pacific (SP) ENSO dynamic afterward, altering its spatial pattern. La Niña was influenced by the SP ENSO dynamic both before and after 1990 and has maintained the CP type. The strengthened SP ENSO dynamic since 1990, accompanied by enhanced precipitation efficiency during La Niña, make it easier for La Niña to transition into MY events. In contrast, there is no observed increase in precipitation efficiency during El Niño.

Plain Language Summary In this study, we explored changes in the El Niño-Southern Oscillation (ENSO) phenomenon from 1950 to 2022. We discovered significant shifts in ENSO complexity, particularly after 1990, affecting where ENSO events occur and how long they last. Notably, these changes differed between El Niño and La Niña phases. El Niño's location shifted from the Eastern Pacific to the Central Pacific, while La Niña extended its duration, leading to more multi-year events. These complexities relate to shifts in El Niño and La Niña dynamics. El Niño changed from a Tropical Pacific dynamic to a Subtropical Pacific dynamic, influencing its shift to the central Pacific. La Niña dynamics remained constant, causing La Niña's central location to remain unchanged. After 1990, the tropical precipitation efficiency showed an asymmetric change between El Niño and La Niña phases. The intensified atmospheric response to La Niña cooling enabled more frequent activations of the SP ENSO dynamic, thus increasing the frequency of multi-year La Niña. These findings advance our understanding of ENSO and can enhance ENSO prediction.

1. Introduction

El Niño-Southern Oscillation (ENSO) is one of the strongest interannual climate variations and can impact worldwide climate (McPhaden et al., 2006; Power et al., 2013). Research since the 1970s has proposed several theories to successfully explain its common properties (e.g., Jin, 1997; Latif et al., 1998; Philander, 1983; Wyrtki, 1985). However, ENSO properties in recent decades differ from those before, leading to increased attention on event-to-event differences, which is referred to as ENSO diversities or complexities (Capotondi et al., 2015; Timmermann et al., 2018).

ENSO complexities manifest at least on three aspects: spatial pattern, temporal evolution, and intensity. ENSO is now divided into Eastern Pacific (EP) and Central Pacific (CP) types (Kao & Yu, 2009; Yu & Kao, 2007) based on the central zonal location of its largest sea surface temperature anomalies (SSTAs) (Ashok et al., 2007; Capotondi et al., 2015; Kug et al., 2009; Larkin & Harrison, 2005). The CP ENSO occurs more frequently in the 21st century, possibly due to global warming (McPhaden et al., 2011; Yeh et al., 2009), natural decadal variability (Yu et al., 2015), or random variability (Newman et al., 2011). ENSO intensity has also fluctuated, increasing after the mid-1970s (An & Wang, 2000) but decreasing in the 21st century (Hu et al., 2020). Regarding temporal evolution, ENSO typically lasts a year, however, some recent ENSO events lasted over a year, becoming multi-year (MY) events, such as the 2014–2016 MY El Niño and the 2020–2023 MY La Niña. These changes suggest evolving ENSO complexities in spatial pattern, temporal evolution, and intensity. We aim to quantify these changes and determine the specific timing of the changes. Additionally, La Niña usually exhibits weaker intensity (Burgers & Stephenson, 1999; Deser & Wallace, 1987), more westward location (Kug & Ham, 2011), and longer

evolution (Larkin & Harrison, 2002; Okumura & Deser, 2010) compared to El Niño. Therefore, we must investigate whether the ENSO complexity changes are asymmetric between El Niño and La Niña phases.

One potential reason for the ENSO complexity changes is shifts in ENSO dynamics. The classic ENSO theory, known as the recharge oscillator (Jin, 1997), referred to the Tropical Pacific (TP) ENSO dynamic, emphasizes thermocline variations along the equatorial Pacific and their lead-lag interactions with surface winds and SSTs. The TP ENSO dynamic favors the SSTAs in the eastern equatorial Pacific, where the SSTs are most sensitive to thermocline variations (Yu et al., 2017). This dynamic promotes single-year (SY) ENSO events (Yu & Fang, 2018) since the El Niño/La Niña-induced zonal winds consistently trigger out-of-phase heat content changes, leading to the termination of the El Niño/La Niña. That is, the TP ENSO dynamic primarily generates EP and SY ENSO, contributing to reduce ENSO complexities.

Recently, another Subtropical Pacific (SP) ENSO dynamic has been proposed (Capotondi et al., 2015; Di Lorenzo et al., 2015; Yu et al., 2010, 2012), which emphasizes that through Wind-Evaporation-SST feedbacks (Xie & Philander, 1994), a North Pacific Meridional Mode (NPMM) (Chiang & Vimont, 2004) can be formed and bring SSTAs from the northeastern subtropical Pacific to the central tropical Pacific (Vimont et al., 2001) to develop a CP ENSO (Yu & Kim, 2011; Yu et al., 2017). Furthermore, a mature ENSO event could provide feedback to the subtropical North Pacific, triggering the next NPMM event. This, in turn, sustains the El Niño/La Niña event through the SP ENSO dynamic, ultimately resulting in a MY ENSO event (Fang & Yu, 2020; Yu & Fang, 2018). That is, the SP ENSO dynamic can lead to greater ENSO complexities. Another goal of this study is to explore if the relative importance of TP and SP ENSO dynamics has changed and whether this dynamic change can explain the ENSO complexity changes.

In brief, we address the following four scientific questions: (a) Have ENSO complexities in spatial pattern, temporal evolution, and intensity and ENSO dynamics changed in recent decades? (b) Can we precisely identify the timing of these changes? (c) Can the changes in ENSO dynamics explain the changes in ENSO complexities? (d) Are these changes asymmetric or symmetric between El Niño and La Niña phases?

2. Data and Methods

This study uses SST from the Hadley Center Sea Ice and SST (Rayner et al., 2003), winds from the National Centers for Environmental Prediction/National Center for Atmospheric Research Reanalysis 1 (Kalnay et al., 1996), sea surface height (SSH) from Ocean Reanalysis System 4 (Balmaseda et al., 2013), subsurface temperature from Institute of Atmospheric Physics (Cheng et al., 2017), precipitation from the National Oceanic and Atmospheric Administration (Chen et al., 2004) (see details in Data Availability Statement). All analyses cover the period 1950–2022, except for SSH data, which spans for 1958–2017. Anomalies are defined as the deviations from the seasonal cycle averaged over the analysis period after removing linear trends.

Besides the Niño indices (Niño4, Niño3.4, Niño1+2 and cold tongue index (CTI)), we also employed the NPMM index to quantify the strength of NPMM and the TP and SP indices to respectively measure the strengths of TP and SP ENSO dynamics (see Text S1 in Supporting Information S1). ENSO events are categorized into EP or CP types based on the relative strength of the Niño1+2 and Niño4 indices, and into SY or MY types according to the value of second-year Niño3.4 index (see Text S2 in Supporting Information S1). In this study, we utilized the depth of the 20°C isotherm (D20) as a proxy for thermocline depth. While alternative approaches, such as the maximum vertical gradient of ocean temperature, have been proposed (e.g., Chen et al., 2015, 2017), the use of D20 is considered practical over the eastern tropical Pacific, given the relatively coarse vertical resolution of existing ocean temperature data. Statistical significance is assessed using a two-tail Student's *t*-test.

3. Results

3.1. Changes in ENSO Complexities

Figures 1a–1c display the SSTA evolution along the equatorial Pacific (5°S–5°N) from 1950 to 2022. Superimposed on the evolution is the longitudinal location of the maximum positive (minimum negative) SSTAs over the equatorial central-to-eastern Pacific (120°E to 80°W). There is a distinct longitudinal shift in the SSTA center around 1990, marked by a significant westward shift of 14° (significant at the 99% confidence level), moving from a mean center at 129°W before 1990 to a mean center at 143°W afterward. We then examined the shift separately for warm and cold episodes (Figures 1d and 1e) and discovered an asymmetric change in central

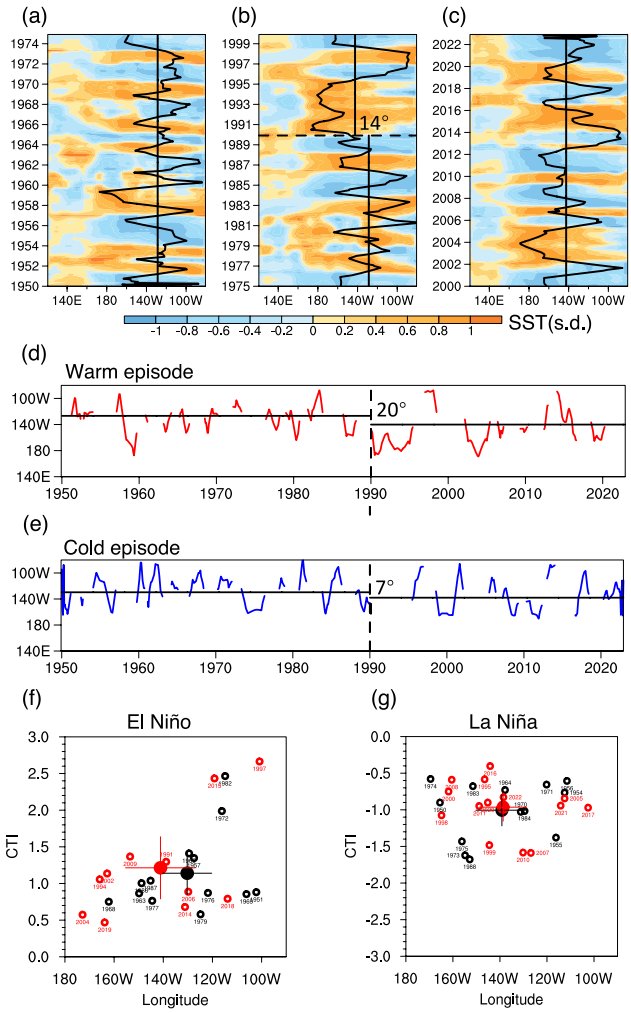

Figure 1. (a–c) Evolution of standardized equatorial (5°S–5°N) SSTA (shading) from 1950 to 2022, smoothed by a 10°-longitude and 10-month running mean. Black lines indicate the longitudinal location of maximum positive (minimum negative) SSTAs over the central-to-eastern Pacific (120°E−80°W). (d–e) Red (blue) lines depict central SSTA locations for warm (cold) episodes in (a–c). Dashed lines in (a–e) separate pre-1990 (1950–1989) and post-1990 (1990–2022) periods. Vertical and horizontal solid-black lines denote mean longitude values of SSTA centers, with numbers indicating specific longitude change values. (f, g) Scatter plot illustrates central location (*X*-axis) and peak intensity (*Y*-axis) of winter (ND^0J^1) SSTAs for El Niño and La Niña events. Hollow (solid) circles represent individual events (mean value), with black (red) circles indicating events before (after) 1990. Numbers next to each hollow circle mark the developing year of the ENSO events. Error bars show 95% confidence intervals.

location, with a more pronounced westward shift of 20° (significant at the 99% confidence level) for warm episode but only 7° for the cold episode. When examining the central location changes specific to El Niño and La Niña (Figures 1f and 1g), El Niño exhibited a conspicuous westward shift of 17° after 1990, while La Niña remained relatively stable. Interestingly, the intensities of both El Niño and La Niña have not undergone profound changes in recent decades, despite earlier suggestions of potential increase in ENSO intensity (Cai et al., 2015; Collins et al., 2010). We also classified the ENSO events into EP and CP types (Table S1 in Supporting Information S1) to investigate whether changes in longitudinal location can cause shifts in ENSO types. El Niño shifted from primarily EP type (61.5%) before 1990 to mostly CP type (63.6%) thereafter (Table S2a in Supporting Information S1). The ratio of the numbers of CP to EP El Niño also increased threefold (0.6–1.8). In contrast, La Niña (Table S2b in Supporting Information S1) remained consistently CP type in both the pre-1990 (53.8%) and the post-1990 (64.2%) periods, with minimal variation in the CP to EP ratio (1.2–1.8). All these analyses highlight a clear shift in the location of El Niño around 1990, whereas the same shift is not observed for La Niña.

We next examined changes in the complexity of ENSO's temporal evolution pattern. Figures 2a and 2b display the composite SSTA evolution along the equatorial Pacific for the pre-1990 and post-1990 El Niño. In both periods, El Niño consistently transitioned into a cold phase in the following year, resulting in an SY evolution pattern. For La Niña, while the pre-1990 La Niña (Figure 2c) tended to persist into the second year, the warm SSTAs from the equatorial eastern Pacific disrupted the central Pacific cooling, interrupting the MY evolution pattern. In contrast, for the post-1990 La Niña (Figure 2d), the cold SSTAs persisted throughout the second year, resulting in a MY event. The different evolution patterns are reflected in the composite Niño3.4 value in the second-year winter (D^1JF^2), which decreased from 0 for the pre-1990 La Niña to −0.33 for the post-1990 La Niña (Figure 2f). Although the Niño3.4 change did not pass 95% significant test (p-value = 0.42), this difference still offers an indication that the duration of La Niña has been elongated after 1990. In contrast, the Niño3.4 values for both the pre-1990 and post-1990 El Niño exhibit similarly negative values (−0.28 and −0.37; Figure 2e), indicating a consistent termination of El Niño events in the second year.

Similarly, we classified individual El Niño and La Niña events as SY or MY events (Table S1 in Supporting Information S1) to investigate whether the changes in the temporal evolution of tropical Pacific SSTAs can project to changes in the frequencies of SY and MY events. El Niño remains dominated by the SY evolution pattern in both pre- and post-1990 periods, with comparable percentages ranging from 53.4% to 63.6% (Table S2a in Supporting Information S1). However, La Niña is consistently characterized by the MY evolution pattern and exhibits a notable increase in dominance percentages after 1990 (61.5%–76.9%; Table S2b in Supporting Information S1). This shift results in a dramatic increase in the ratio of MY to SY for La Niña between these two periods (1.6–3.3). In contrast, the MY to SY ratio decreases moderately for El Niño (0.9–0.6). Therefore, the temporal evolution changes are also asymmetric between El Niño and La Niña phases, with a significant shift toward more MY La Niña after 1990 but no similar trend for El Niño.

3.2. Changes in ENSO Dynamics

To understand the changes in ENSO complexities, we investigated potential modifications in ENSO dynamics since 1990. The TP ENSO dynamic typically associates with the EP and SY ENSO patterns, while the SP ENSO

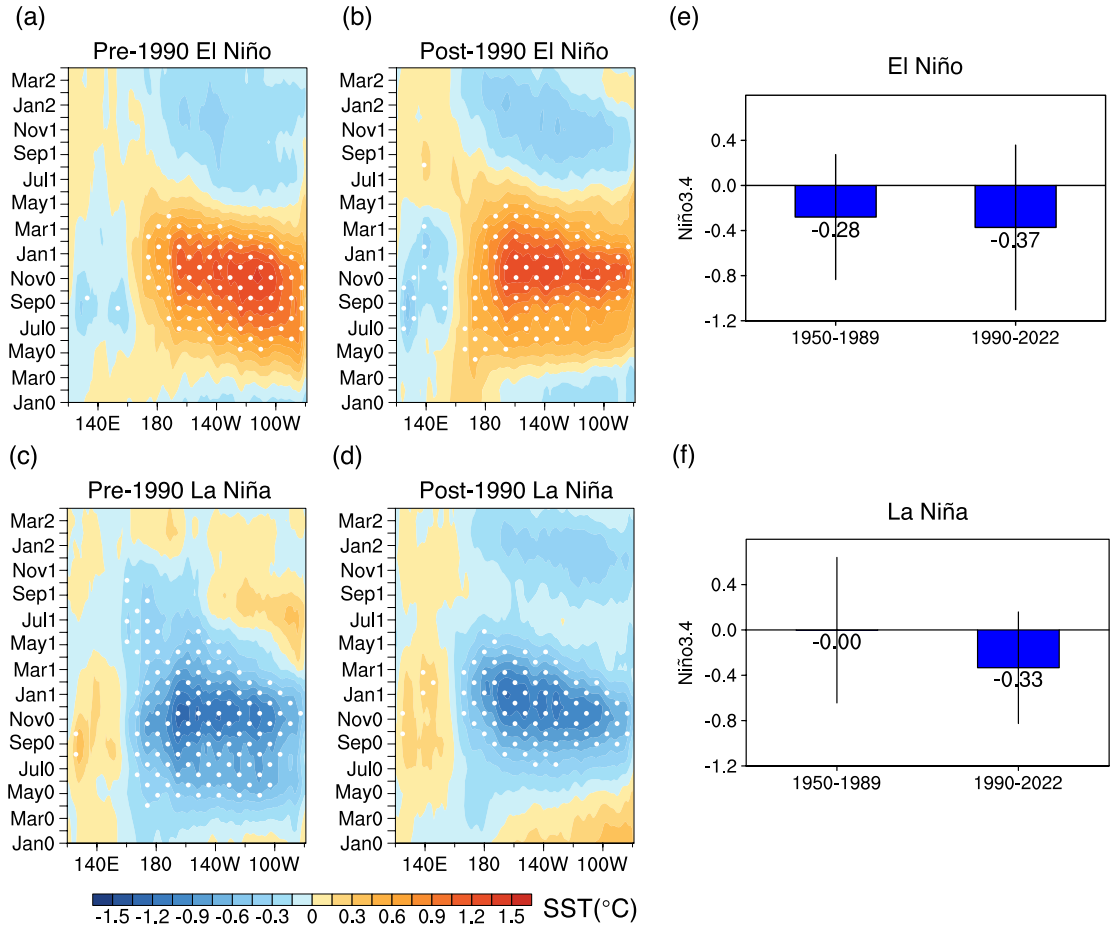

Figure 2. Equatorial (5°S–5°N) SSTA evolution composited for the pre- and post-1990 (a, b) El Niños and (c, d) La Niñas. White dots mark SSTAs significant at the 95% confidence level. Blue bars display mean Niño3.4 values in the second-year winter (ND^1J^2) of pre- and post-1990 (e) El Niños and (f) La Niñas. Error bars represent 95% confidence intervals.

dynamic contributes to CP and MY ENSO events (Yu et al., 2017; Yu & Fang, 2018). We find a significant intensification of subtropical coupling after 1990 (Figure 3a), measured by the 21-year sliding correlation between the February^0-March^0-April^0 (FMA^0) NPMM-Wind index and March^0-April^0-May^0 (MAM^0) NPMM-SST index. The mean coupling strength increased from 0.71 to 0.89 after 1990 (significant at the 95% confidence level; Figure 3b). The intensity of the subtropical coupling-induced NPMM (the variance of the MAM^0 NPMM-SST index) also increased significantly after 1990 (exceeding 90% confidence level; Figure 3c).

The effectiveness of the subtropical coupling in inducing ENSO events, measured by the correlation between boreal spring NPMM-SST index and following winter (November^0-December^0-January^1, ND^0J^1) CTI index (Figure 3d), increased significantly from 0.18 to 0.54 after 1990 (significant at 90% confidence level). Figure S3 in Supporting Information S1 shows the lagged regressions of SSTAs and surface wind anomalies onto the boreal spring NPMM-SST index. In the pre-1990 period, the subtropical Pacific SSTAs induced by the boreal spring NPMM could not reach the tropics (Figures S3a–S3f in Supporting Information S1). However, in the post-1990 period, these SSTAs extended into the tropical central Pacific (Figures S3g–S3l in Supporting Information S1). When these SSTAs reached the tropics, a CP ENSO event emerges in MAM^0, which develops and peaks in subsequent seasons. However, the effectiveness of TP ENSO dynamic in inducing ENSO events, represented by the correlation between MAM^0 mean thermocline depth (D20) over equatorial Pacific (5°S–5°N, 120°E–90°W) and the following ND^0J^1 CTI index (Figure S4 in Supporting Information S1), exhibited little change before and after 1990 (0.57–0.48). Lagged regressions of SSTAs and surface wind anomalies onto the boreal spring D20

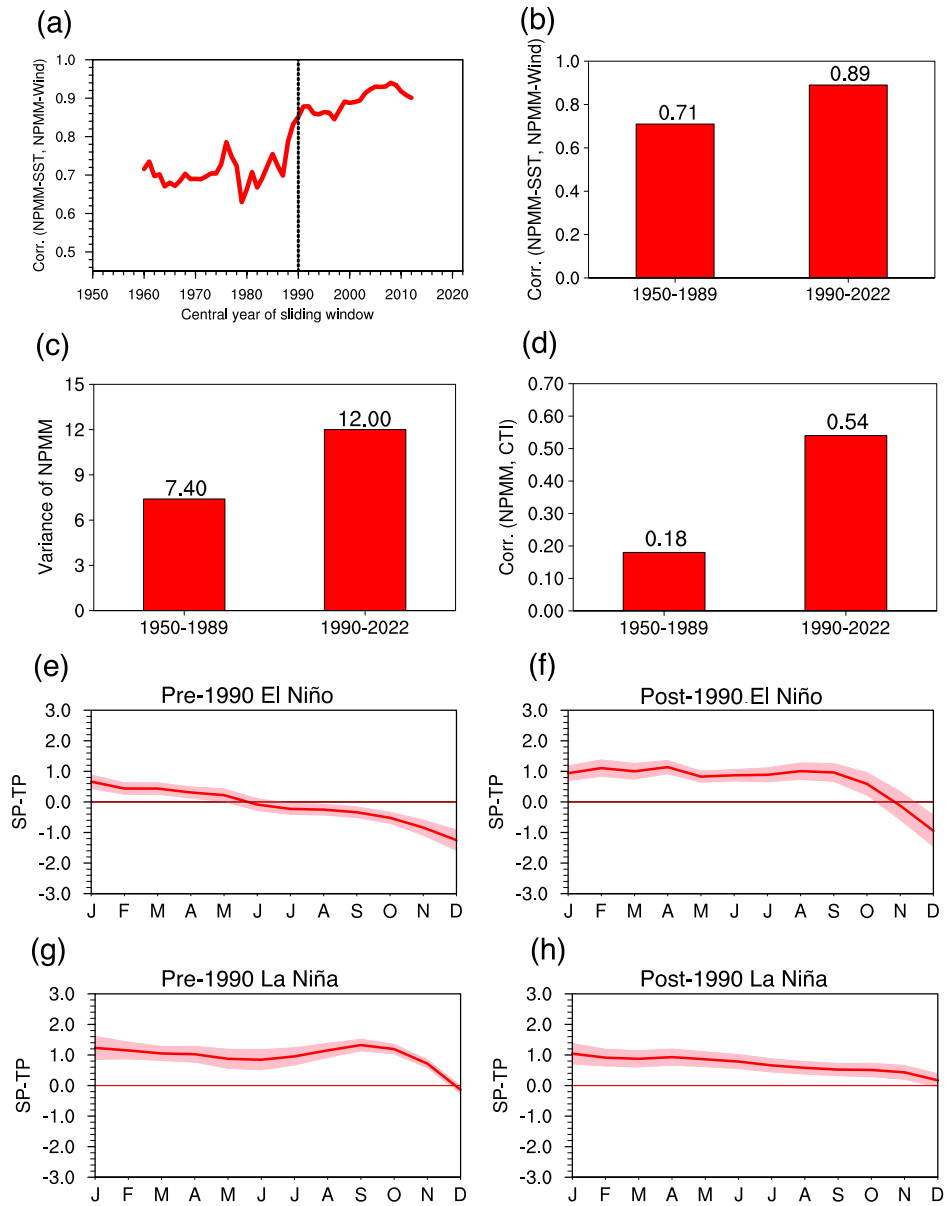

Figure 3. (a) 21-year sliding correlations between FMA^0 NPMM-Wind index and MAM^0 NPMM-SST index. (b) Correlations in (a) separated into pre-1990 and post-1990 periods. (c) Variance of MAM^0 NPMM-SST index in both periods. (d) Correlations between MAM^0 NPMM-SST index and following ND^{0}J^1 CTI in both periods. Composite difference between standardized SP and TP indices for (e) pre-1990 El Niños and (f) post-1990 El Niños. (g, h) Similar to (e, f), but for La Niñas, with differences multiplied by −1 for relative strength assessment. Pink shading bands represent 95% confidence intervals.

further indicated minimal changes in the ability of TP ENSO dynamic to induce ENSO (Figure S5 in Supporting Information S1).

We used the TP and SP indices, obtained through Multivariate Empirical Orthogonal Function (MEOF) analysis on combined SST, wind, and SSH anomalies (Yu & Fang, 2018; see Text S1 for details), to quantify the strengths of the TP and SP ENSO dynamics, respectively. The ratio of the standard deviation of the SP index to that of the TP index increased from 0.95 to 1.14 (Figure S6 in Supporting Information S1). This shift suggests that the SP ENSO dynamic became more influential than TP ENSO dynamic after 1990 on overall ENSO variability. We next separately examined the differences in TP and SP indices of El Niño and La Niña events, both in the periods before and after 1990 (Figures 3e–3h). El Niños were predominantly influenced by the TP ENSO dynamic

throughout their lifecycles before 1990 except the onset phase (Figure 3e), but entirely dominated by the SP ENSO dynamic after 1990 (Figure 3f). In contrast, La Niñas were consistently dominated by the SP ENSO dynamic throughout their lifecycles, both before and after 1990 (Figures 3g and 3h).

3.3. Causes of El Niño-La Niña Asymmetries in Complexity and Dynamic Changes

Comparing the SSTAs regressed onto the NPMM index (Figure S3 in Supporting Information S1) and the D20 index (Figure S5 in Supporting Information S1), we observed that SSTAs in the eastern tropical Pacific exhibit higher sensitivity to thermocline variations, whereas SSTAs in the central tropical Pacific respond more to NPMM fluctuations. In essence, the TP ENSO dynamic promotes EP ENSO, while the SP ENSO dynamic favors CP ENSO. Considering the changed dynamics of El Niño, it should primarily exhibit EP type before 1990 but shift toward CP type after 1990 due to heightened dominance of SP ENSO dynamic. Given that La Niña was consistently governed by the SP ENSO dynamic, its spatial pattern should maintain the CP type. Consequently, the contrasting predominance of TP and SP ENSO dynamics explains the El Niño-La Niña asymmetry in ENSO complexity changes in spatial patterns.

The further question is why El Niño and La Niña were dominated by different ENSO dynamics during the pre-1990 period, but shifted to the same SP ENSO dynamic after 1990? The asymmetry in El Niño and La Niña dynamics is attributed to present-day climate conditions with a relatively shallow eastern equatorial thermocline. The cold ocean temperature below the thermocline is partially reflected in climatological SSTs in the eastern equatorial Pacific, limiting further cooling despite increased thermocline lifting. In contrast, a deepened thermocline hinders the below-thermocline cold ocean temperature from reaching the surface, resulting in significant warming of equatorial eastern Pacific SSTs. This asymmetric impact is demonstrated by more pronounced SST warming during deeper thermocline years (Figure S7a in Supporting Information S1) compared to shallower years (Figure S7b in Supporting Information S1). The TP ENSO dynamic, characterized by equatorial Pacific thermocline deepening and lifting, is more effective in inducing El Niño but less efficient in inducing La Niña, with the latter consistently influenced by the SP ENSO dynamic. Through a 21-year running analysis (Figure S8 in Supporting Information S1), we observed a significant deepening of the mean thermocline from the pre-1990 to the post-1990 periods, indicating a 6.9% over the tropical eastern Pacific (5°S–5°N and 90°–80°W; Figure S9a in Supporting Information S1) and a 16.7% over the Niño1+2 region (Figure S9b in Supporting Information S1). This deepening weakens the importance of thermocline feedback on SSTAs, diminishing the significance of the TP ENSO dynamic on El Niño after 1990. Therefore, after 1990, the TP ENSO dynamic relinquished its dominant position to the SP ENSO dynamic in influencing El Niño activities.

Another asymmetry in the evolution of El Niño-La Niña complexity is the heightened prevalence of MY La Niña events compared to MY El Niño events after 1990. As previously mentioned, the SP ENSO dynamic facilitates the emergence of MY ENSO events. For a subsequent same-phase event to be triggered through this SP ENSO dynamic, a mature ENSO event needs to induce significant heating (precipitation) anomalies over the central tropical Pacific, thereby exciting an atmospheric wave to the subtropical Pacific and triggering the SP ENSO dynamic (Fang & Yu, 2020; Yu & Fang, 2018). We noticed that although the post-1990 El Niño SSTAs over the central tropical Pacific increased compared to the pre-1990 one (0.24°C–0.39°C; Table S3 in Supporting Information S1), the precipitation anomalies during their peak season (ND^0J^1) are nearly comparable (1.24 mm d^{-1} and 1.46 mm d^{-1}; Figures 4a and 4b; Table S3 in Supporting Information S1). This suggests that post-1990 El Niño exhibited decreased precipitation efficiency (5.22 mm $d^{-1}°C^{-1}$ to 3.79 mm $d^{-1}°C^{-1}$; Table S3 in Supporting Information S1), likely due to convective insensitivity once SSTs exceeded the threshold (Graham & Barnett, 1987). This decreased tropical heating efficiency limited the second-year SP ENSO dynamic of post-1990 El Niño and therefore fewer MY events.

In contrast, the negative precipitation anomalies of La Niña in the central tropical Pacific (Figures 4c and 4d) intensified significantly after 1990 (−1.12 mm d^{-1} to −1.91 mm d^{-1}; Table S3 in Supporting Information S1). Unlike El Niño, the La Niña SSTAs intensity in that region showed a slightly change between the two periods (−0.39°C to −0.43°C; Table S3 in Supporting Information S1). Therefore, the post-1990 La Niña exhibits higher precipitation efficiency (2.90 mm $d^{-1}°C^{-1}$ to 4.48 mm $d^{-1}°C^{-1}$; Table S3 in Supporting Information S1). The intensified precipitation response equips post-1990 La Niña with greater capability to activate the SP ENSO dynamic, thus facilitating the occurrence of MY events. The more likely SP ENSO dynamic, combined with its increased strength, together contribute to the increased frequency of MY La Niña events compared to the pre-1990 period.

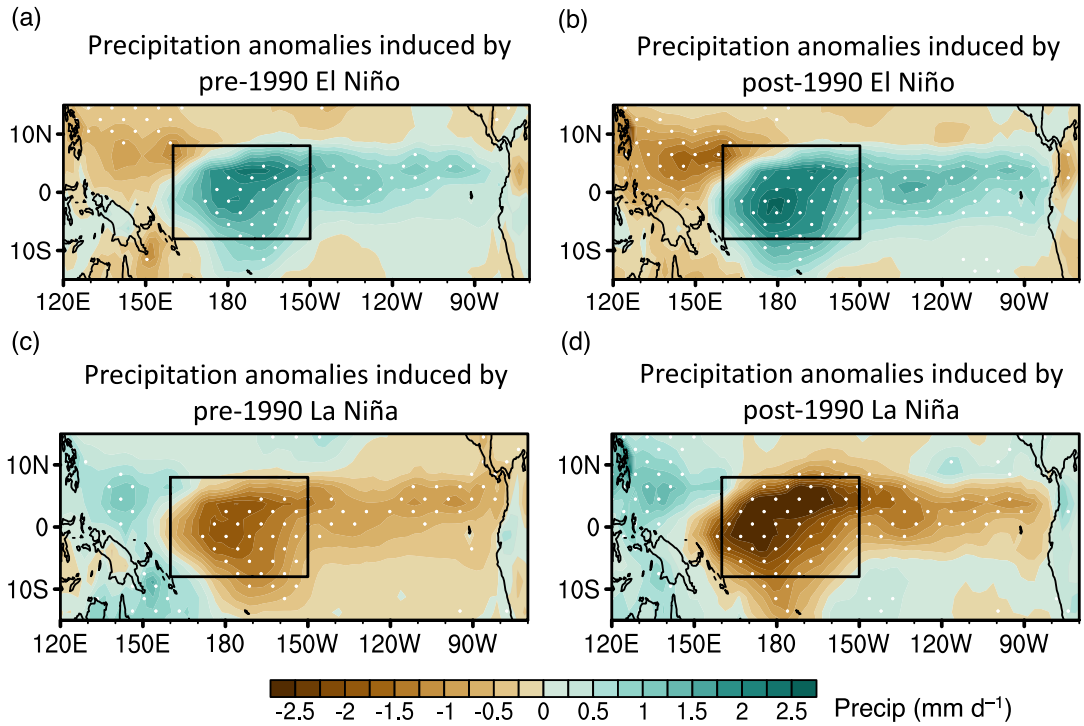

Figure 4. Composite precipitation anomalies in El Niños during the (a) pre-1990 period and (b) post-1990 period. (c, d) As in (a, b), but for La Niñas. White dots indicate significant precipitation anomalies at the 95% confidence level. Black boxes represent the central tropical Pacific region (8°S–8°N, 160°E−150°W) where the precipitation and SST anomalies are calculated and listed in Table S3 in Supporting Information S1.

4. Summary and Discussion

In this study, we observed asymmetric changes in ENSO complexity in spatial pattern and temporal evolution from 1950 to 2022. El Niño shifted its spatial pattern westward from EP to CP type after 1990, while La Niña extended its temporal evolution, leading to more frequent MY events after 1990. ENSO dynamics accordingly showed apparent changes around 1990, with the SP ENSO dynamic strengthened distinctively after 1990, while the TP ENSO dynamic weakened slightly. The intensified SP ENSO dynamic played an important role in the westward location shift of El Niño, and increased the occurrence of MY La Niña events together with the intensified precipitation. Our findings highlight the necessity of separating El Niño and La Niña when examining ENSO complexities and dynamics.

It is known that CP El Niño usually manifests with lower intensity compared to the EP El Niño. Given the increased occurrence of CP El Niño in the post-1990 period, one might expect a corresponding decrease in the overall intensity of El Niño. However, as shown in Figure 1f, there are no significant changes in El Niño intensity before and after 1990. The consistent mean intensity can be attributed to the occurrence of three extreme El Niño events (1982/83, 1997/98, 2015/16). Previous studies (e.g., Cai et al., 2014) argue that extreme El Niño events exhibit different ENSO dynamics from other El Niños. If we repeat the Figure 1f analysis but exclude these three extreme El Niño events, the mean intensity of El Niño decreases from 1.21°C in the pre-1990 period to 0.92°C in the post-1990 period (Figure S10 in Supporting Information S1). After 1990, the dominated CP El Niños did exhibit lower intensity compared to the EP-dominated El Niños observed before 1990.

There are several issues require further investigation. A noteworthy issue is the asymmetric trend in precipitation efficiency between El Niño and La Niña before and after 1990. One possible explanation for this asymmetry could be the increase in tropical convective threshold due to global warming. According to Johnson and Xie (2010), there is an increasing trend of approximately 0.1°C/decade in the convective threshold in the tropics during the period 1980–2010. In the present-day tropical central Pacific conditions, where mean SSTs can trigger deep convection, local SSTs likely already surpass the convection threshold. During the post-1990 period, the

presumed higher convective threshold value may facilitate La Niña events in more easily reducing local SSTs below the threshold, leading to a negative precipitation anomaly. In contrast, the pre-1990 period, presumed to have a lower convective threshold, may limit the capability of La Niña cooling to bring down local SSTs sufficiently below the convective threshold, resulting in less pronounced negative precipitation anomalies compared to the post-1990 period. As a result, La Niña events might demonstrate an enhanced ability to induce negative precipitation anomalies in the post-1990 period compared to the pre-1990 period, owing to the modified convective threshold values. In contrast, El Niño events elevate SSTs over the tropical central Pacific, which already surpass the convective threshold. Consequently, the positive precipitation anomaly induced by El Niño events is expected to remain consistent before and after the 1990s. Therefore, there is no change in the precipitation efficiency produced by El Niño events between these two periods.

Also, the specific reasons for ENSO complexities and dynamics changes around 1990 remained debated. Previous studies linked causes to factors such as the Atlantic Meridional Oscillation (Lyu et al., 2017; Yu et al., 2015), North Atlantic Oscillation (Ding et al., 2023), global warming (Ashok et al., 2007; Yeh et al., 2009), or even deforestation in the Maritime Continent (Lee et al., 2023). However, further studies are required for comprehensive understanding of the underlying causes.

Data Availability Statement

The Hadley Center Sea Ice and SST data is available at Rayner et al. (2003). The National Centers for Environmental Prediction/National Center for Atmospheric Research Reanalysis 1 data are available at Kalnay et al. (1996). The Ocean Reanalysis System 4 data is available at Balmaseda et al. (2013). The Institute of Atmospheric Physics subsurface temperature data is available at Cheng et al. (2017). The NPMM indices are available at Chiang and Vimont (2004).

Acknowledgments
This research was supported by the Climate and Large-Scale Dynamics Program of the U. S. National Science Foundation under Grants AGS-2109539.

References

An, S.-I., & Wang, B. (2000). Interdecadal change of the structure of the ENSO mode and its impact on the ENSO frequency. *Journal of Climate*, *13*(12), 2044–2055. https://doi.org/10.1175/1520-0442(2000)013<2044:ICOTSO>2.0.CO;2

Ashok, K., Behera, S. K., Rao, S. A., Weng, H., & Yamagata, T. (2007). El Niño Modoki and its possible teleconnection. *Journal of Geophysical Research*, *112*(C11), C11007. https://doi.org/10.1029/2006jc003798

Balmaseda, M. A., Mogensen, K., & Weaver, A. T. (2013). Evaluation of the ECMWF ocean reanalysis system ORAS4 [Dataset]. *Quarterly Journal of the Royal Meteorological Society*, *139*, 1132–1161. https://doi.org/10.1002/qj.2063

Burgers, G., & Stephenson, D. B. (1999). The "normality" of El Niño. *Geophysical Research Letters*, *26*(8), 1027–1030. https://doi.org/10.1029/1999GL900161

Cai, W., Borlace, S., Lengaigne, M., van Rensch, P., Collins, M., Vecchi, G., et al. (2014). Increasing frequency of extreme El Niño events due to greenhouse warming. *Nature Climate Change*, *4*(2), 111–116. https://doi.org/10.1038/nclimate2100

Cai, W., Santoso, A., Wang, G., Yeh, S.-W., An, S.-I., Cobb, K. M., et al. (2015). ENSO and greenhouse warming. *Nature Climate Change*, *5*(9), 849–859. https://doi.org/10.1038/nclimate2743

Capotondi, A., Wittenberg, A. T., Newman, M., Lorenzo, E. D., Yu, J.-Y., Braconnot, P., et al. (2015). Understanding ENSO diversity. *Bulletin of the American Meteorological Society*, *96*(6), 921–938. https://doi.org/10.1175/BAMS-D-13-00117.1

Chen, L., Li, T., & Yu, Y. (2015). Causes of strengthening and weakening of ENSO amplitude under global warming in four CMIP5 models. *Journal of Climate*, *28*(8), 3250–3274. https://doi.org/10.1175/JCLI-D-14-00439.1

Chen, L., Li, T., Yu, Y., & Behera, S. K. (2017). A possible explanation for the divergent projection of ENSO amplitude change under global warming. *Climate Dynamics*, *49*(11–12), 3799–3811. https://doi.org/10.1007/s00382-017-3544-x

Chen, M., Xie, P., Janowiak, J. E., Arkin, P. A., & Smith, T. M. (2004). Verifying the reanalysis and climate models outputs using a 56-year data set of reconstructed global precipitation. In *14th AMS Conference on Applied Meteorology*.

Cheng, L., Trenberth, K. E., Fasullo, J., Boyer, T., Abraham, J., & Zhu, J. (2017). Improved estimates of ocean heat content from 1960 to 2015 [Dataset]. *Science Advances*, *3*. e1601545. https://doi.org/10.1126/sciadv.1601545

Chiang, J. C. H., & Vimont, D. J. (2004). Analogous Pacific and Atlantic meridional modes of tropical atmosphere–ocean variability [Dataset]. *Journal of Climate*, *17*, 4143–4158. https://doi.org/10.1175/JCLI4953.1

Collins, M., An, S.-I., Cai, W., Ganachaud, A., Guilyardi, E., Jin, F.-F., et al. (2010). The impact of global warming on the tropical Pacific Ocean and El Niño. *Nature Geoscience*, *3*(6), 391–397. https://doi.org/10.1038/ngeo868

Deser, C., & Wallace, J. M. (1987). El Niño events and their relation to the Southern oscillation: 1925–1986. *Journal of Geophysical Research*, *92*(C13), 14189–14196. https://doi.org/10.1029/JC092iC13p14189

Di Lorenzo, E., Liguori, G., Schneider, N., Furtado, J. C., Anderson, B. T., & Alexander, M. A. (2015). ENSO and meridional modes: A null hypothesis for Pacific climate variability. *Geophysical Research Letters*, *42*(21), 9440–9448. https://doi.org/10.1002/2015GL066281

Ding, R., Nnamchi, H. C., Yu, J.-Y., Li, T., Sun, C., Li, J., et al. (2023). North Atlantic oscillation controls multidecadal changes in the North tropical Atlantic–Pacific connection. *Nature Communications*, *14*(1), 862. https://doi.org/10.1038/s41467-023-36564-3

Fang, S.-W., & Yu, J.-Y. (2020). A control of ENSO transition complexity by tropical Pacific mean SSTs through tropical-subtropical interaction. *Geophysical Research Letters*, *47*(12), e2020GL087933. https://doi.org/10.1029/2020gl087933

Graham, N. E., & Barnett, T. P. (1987). Sea surface temperature, surface wind divergence, and convection over tropical oceans. *Science*, *238*(4827), 657–659. https://doi.org/10.1126/science.238.4827.657

Hu, Z.-Z., Kumar, A., Huang, B., Zhu, J., L'Heureux, M., McPhaden, M. J., & Yu, J.-Y. (2020). The interdecadal shift of ENSO properties in 1999/2000: A review. *Journal of Climate*, *33*(11), 4441–4462. https://doi.org/10.1175/JCLI-D-19-0316.1

Jin, F.-F. (1997). An equatorial ocean recharge paradigm for ENSO. Part I: Conceptual model. *Journal of the Atmospheric Sciences*, *54*(7), 811–829. https://doi.org/10.1175/1520-0469(1997)054<0811:AEORPF>2.0.CO;2

Johnson, N. C., & Xie, S.-P. (2010). Changes in the sea surface temperature threshold for tropical convection. *Nature Geoscience*, *3*(12), 842–845. https://doi.org/10.1038/ngeo1008

Kalnay, E., Kanamitsu, M., Kistler, R., Collins, W., Deaven, D., Gandin, L., et al. (1996). The NCEP/NCAR 40-year reanalysis project [Dataset]. *Bulletin of the American Meteorological Society*, *77*, 437–472. https://doi.org/10.1175/1520-0477(1996)077<0437:TNYRP>2.0.CO;2

Kao, H.-Y., & Yu, J.-Y. (2009). Contrasting eastern-Pacific and central-Pacific types of ENSO. *Journal of Climate*, *22*(3), 615–632. https://doi.org/10.1175/2008JCLI2309.1

Kug, J.-S., & Ham, Y.-G. (2011). Are there two types of La Nina? *Geophysical Research Letters*, *38*(16), L16704. https://doi.org/10.1029/2011GL048237

Kug, J.-S., Jin, F.-F., & An, S.-I. (2009). Two types of El Niño events: Cold tongue El Niño and warm pool El Niño. *Journal of Climate*, *22*(6), 1499–1515. https://doi.org/10.1175/2008JCLI2624.1

Larkin, N. K., & Harrison, D. E. (2002). ENSO warm (El Niño) and cold (La Niña) event life cycles: Ocean surface anomaly patterns, their symmetries, asymmetries, and implications. *Journal of Climate*, *15*(10), 1118–1140. https://doi.org/10.1175/1520-0442(2002)015<1118:EWENOA>2.0.CO;2

Larkin, N. K., & Harrison, D. E. (2005). On the definition of El Niño and associated seasonal average US weather anomalies. *Geophysical Research Letters*, *32*(13), L13705. https://doi.org/10.1029/2005gl022738

Latif, M., Anderson, D., Barnett, T., Cane, M., Kleeman, R., Leetmaa, A., et al. (1998). A review of the predictability and prediction of ENSO. *Journal of Geophysical Research*, *103*(C7), 14375–14393. https://doi.org/10.1029/97JC03413

Lee, T.-H., Yu, J.-Y., Lin, Y.-F., Lo, M.-H., & Xiao, H.-M. (2023). The potential influence of maritime continent deforestation on El Niño-Southern Oscillation: Insights from idealized modeling experiments. *Geophysical Research Letters*, *50*(20), e2023GL105012. https://doi.org/10.1029/2023GL105012

Lyu, K., Yu, J.-Y., & Paek, H. (2017). The influences of the Atlantic multidecadal oscillation on the mean strength of the North Pacific subtropical high during boreal winter. *Journal of Climate*, *30*(1), 411–426. https://doi.org/10.1175/JCLI-D-16-0525.1

McPhaden, M. J., Lee, T., & McClurg, D. (2011). El Niño and its relationship to changing background conditions in the tropical Pacific Ocean. *Geophysical Research Letters*, *38*(15), L15709. https://doi.org/10.1029/2011gl048275

McPhaden, M. J., Zebiak, S. E., & Glantz, M. H. (2006). ENSO as an integrating concept in Earth science. *Science*, *314*(5806), 1740–1745. https://doi.org/10.1126/science.1132588

Newman, M., Shin, S.-I., & Alexander, M. A. (2011). Natural variation in ENSO flavors. *Geophysical Research Letters*, *38*(14), L14705. https://doi.org/10.1029/2011GL047658

Okumura, Y. M., & Deser, C. (2010). Asymmetry in the duration of El Niño and La Niña. *Journal of Climate*, *23*(21), 5826–5843. https://doi.org/10.1175/2010JCLI3592.1

Philander, S. G. H. (1983). El Niño Southern oscillation phenomena. *Nature*, *302*(5906), 295–301. https://doi.org/10.1038/302295a0

Power, S., Delage, F., Chung, C., Kociuba, G., & Keay, K. (2013). Robust twenty-first-century projections of El Niño and related precipitation variability. *Nature*, *502*(7472), 541–545. https://doi.org/10.1038/nature12580

Rayner, N. A. A., Parker, D. E., Horton, E. B., Folland, C. K., Alexander, L. V., Rowell, D. P., et al. (2003). Global analyses of sea surface temperature, sea ice, and night marine air temperature since the late nineteenth century [Dataset]. *Journal of Geophysical Research*, *108*, 4407. https://doi.org/10.1029/2002JD002670

Timmermann, A., An, S.-I., Kug, J.-S., Jin, F.-F., Cai, W., Capotondi, A., et al. (2018). El Niño–Southern oscillation complexity. *Nature*, *559*(7715), 535–545. https://doi.org/10.1038/s41586-018-0252-6

Vimont, D. J., Battisti, D. S., & Hirst, A. C. (2001). Footprinting: A seasonal connection between the tropics and mid-latitudes. *Geophysical Research Letters*, *28*(20), 3923–3926. https://doi.org/10.1029/2001GL013435

Wyrtki, K. (1985). Water displacements in the Pacific and the genesis of El Nino cycles. *Journal of Geophysical Research*, *90*(C4), 7129–7132. https://doi.org/10.1029/JC090iC04p07129

Xie, S., & Philander, S. G. H. (1994). A coupled ocean-atmosphere model of relevance to the ITCZ in the eastern Pacific. *Tellus*, *46*(4), 340–350. https://doi.org/10.1034/j.1600-0870.1994.t01-1-00001.x

Yeh, S.-W., Kug, J.-S., Dewitte, B., Kwon, M.-H., Kirtman, B. P., & Jin, F.-F. (2009). El Niño in a changing climate. *Nature*, *461*(7263), 511–514. https://doi.org/10.1038/nature08316

Yu, J.-Y., & Fang, S.-W. (2018). The distinct contributions of the seasonal footprinting and charged-discharged mechanisms to ENSO complexity. *Geophysical Research Letters*, *45*(13), 6611–6618. https://doi.org/10.1029/2018gl077664

Yu, J.-Y., & Kao, H.-Y. (2007). Decadal changes of ENSO persistence barrier in SST and ocean heat content indices: 1958–2001. *Journal of Geophysical Research*, *112*(D13), D13106. https://doi.org/10.1029/2006jd007654

Yu, J.-Y., Kao, H.-Y., & Lee, T. (2010). Subtropics-related interannual sea surface temperature variability in the central equatorial Pacific. *Journal of Climate*, *23*(11), 2869–2884. https://doi.org/10.1175/2010JCLI3171.1

Yu, J.-Y., Kao, P., Paek, H., Hsu, H.-H., Hung, C., Lu, M.-M., & An, S.-I. (2015). Linking emergence of the central Pacific El Niño to the Atlantic multidecadal oscillation. *Journal of Climate*, *28*(2), 651–662. https://doi.org/10.1175/JCLI-D-14-00347.1

Yu, J.-Y., & Kim, S. T. (2011). Relationships between extratropical sea level pressure variations and the central Pacific and eastern Pacific types of ENSO. *Journal of Climate*, *24*(3), 708–720. https://doi.org/10.1175/2010JCLI3688.1

Yu, J.-Y., Lu, M.-M., & Kim, S. T. (2012). A change in the relationship between tropical central Pacific SST variability and the extratropical atmosphere around 1990. *Environmental Research Letters*, *7*(3), 034025. https://doi.org/10.1088/1748-9326/7/3/034025

Yu, J.-Y., Wang, X., Yang, S., Paek, H., & Chen, M. (2017). The changing El Niño–Southern Oscillation and associated climate extremes. *Climate Extremes: Patterns and Mechanisms*, 1–38.